

Mechanisms of carriers transport in Ni/n-SiC, Ti/n-SiC ohmic contacts

R. KISIEL^{1*}, M. GUZIEWICZ², K. GOLASZEWSKA², M. SOCHACKI¹, W. PASZKOWICZ³

¹ Warsaw University of Technology, Institute of Microelectronics and Optoelectronics,
ul. Koszykowa 75, 00-662 Warszawa, Poland

² Institute of Electron Technology, Al. Lotników 32/46, 02-668 Warszawa, Poland

³ Institute of Physics, Polish Academy of Science, Al. Lotników 32/46, 02-668 Warszawa, Poland

A mechanism of carriers transport through metal-semiconductor interface created by nickel or titanium-based ohmic contacts on Si-face n-type 4H-SiC is presented herein. The mechanism was observed within the temperature range of 20 °C ÷ 300 °C which are typical for devices operating at high current density and at poor cooling conditions. It was found that carriers transport depends strongly on concentration of dopants in the epitaxial layer. The carriers transport has thermionic emission nature for low dopant concentration of $5 \times 10^{16} \text{ cm}^{-3}$. The thermionic emission was identified for moderate dopant concentration of $5 \times 10^{17} \text{ cm}^{-3}$ at temperatures higher than 200 °C. Below 200 °C, the field emission dominates (for the same doping level of $5 \times 10^{17} \text{ cm}^{-3}$). High dopant concentration of $5 \times 10^{18} \text{ cm}^{-3}$ leads to almost pure field emission transport within the whole investigated temperature range.

Keywords: SiC, ohmic contact, carrier transport, silicide, carbide

© Wrocław University of Technology.

1. Introduction

A lot of technical issues should be overcome for improvement of SiC-based power devices performance. One of them is the reproducible formation of thermally-stable ohmic contact. Numerous metals such as Ni, Ti, W, Mo, Co and Ta were studied as materials for fabrication of the ohmic contact to n-type SiC [1, 2]. Nickel and titanium are frequently applied for this purpose. Nickel metallization is commonly applied due to the lowest specific contact resistance (r_c) of ohmic contact. Titanium is still promising and investigated because the ohmic contacts to both n- and p-type SiC can potentially be formed in a single process.

Full understanding of the mechanism of carrier transport through metal and silicon carbide interface working within temperature range of 20 °C ÷ 300 °C is necessary for the development and production of high power and high temperature SiC devices. The electrical properties of the interface will be satisfying when the ohmic contacts are cha-

racterized by extremely low contact resistivity (r_c). The contact resistivity is often highly sensitive to semiconductor dopant concentration. The carriers transport through the given metal-semiconductor (m-s) junction relies on one or more of three phenomena: thermionic emission, thermal field emission and field emission [3].

The thermionic emission is related to the carriers transport above the barrier created at m-s junction. Thermal field emission is a result of carriers flow through the barrier top. The field emission is based on the transition of carriers through the barrier located close to the Fermi level. A way of the emission classification was introduced by Padovani and Stratton [4]. These authors have proposed to use for this purpose the so called tunneling indicator (E_{00}) that depends on the doping level:

$$E_{00} = \frac{h}{4\pi} \sqrt{\frac{N_D}{\epsilon_S \epsilon_0 m^*}} \quad (1)$$

where: ϵ_S is the relative permittivity of the semiconductor, ϵ_0 is the free-space permittivity, N_D is the concentration of active dopants (donors), m^* is an

*E-mail: rkisiel@elka.pw.edu.pl

effective electron mass in the semiconductor, h is Planck constant.

The value of the tunneling indicator E_{00} describes the range of dopant concentrations at which carriers can be transported according to thermionic, thermal field or field emission. The thermionic emission dominates at low concentrations ($E_{00} \ll kT$), thermal field emission at medium concentrations ($E_{00} \approx kT$) and field emission at high concentrations ($E_{00} \gg kT$) [5]. The specific contact resistance for thermionic emission is defined as [5]:

$$r_c = \frac{k}{qTA^*} \exp \left[\frac{-q(\phi_B - \Delta\phi_B)}{kT} \right] \quad (2)$$

where: k is the Boltzmann constant, q is electron charge, T is absolute temperature, A^* is the effective Richardson constant, ϕ_B is the potential barrier height, $\Delta\phi_B$ is a decrease in the potential barrier height due to the mirror-image forces.

The contact resistivity is strongly temperature dependent for thermionic emission. It means that the r_c dependence versus $1/T$ is linear on a semi logarithmic scale with the slope proportional to the barrier height ϕ_B . The barrier height can be mainly

reduced by thermal treatment of the ohmic contact. The high temperature annealing process leads to solid state chemical reaction between metal and semiconductor. As a result of the annealing process, some metal silicides, metal carbides, ternary phases or their mixtures [6], carbon clusters or inclusions described by non-uniform distribution as well as voids can be formed in the transition layer [7]. The carbon atoms are able to segregate as graphite-like interstitial film and create donor-like vacancies in the subsurface region [8].

The contact resistivity for thermal field emission is proportional to the exponential expression given in ref. [5]:

$$r_c \propto \left[\frac{\phi_B}{E_{00} \coth \left[\frac{E_{00}}{kT} \right]} \right] \quad (3)$$

The contact resistivity increases as temperature is decreased but the dependence is weaker comparing to the case of thermionic emission changes which is specific for thermal field emission transport.

The field emission theory gives the following relationship for the contact resistivity [5]:

$$r_c \approx \frac{kT\sqrt{E_{00}}}{qT^2A^*\sqrt{V_dq}} \exp \left[\frac{V_dq}{E_\infty} \right] \times \exp \left[\frac{\phi_F}{kT} \right] \propto \exp \left[\frac{2\sqrt{\epsilon_S\epsilon_0m^*}}{\hbar} \frac{\phi_B}{\sqrt{N_D}} \right] \quad (4)$$

where V_d is diffusion potential, N_D is donor concentration.

When the field emission is the dominating transport mechanism, the contact resistivity will be virtually independent of temperature.

In this paper, the study of carriers transport through metal-semiconductor interface fabricated on Si-face n-type 4H-SiC by nickel or titanium deposition followed by annealing is presented.

2. Experimental

The 3 μm -thick n-type epitaxial layers deposited on 4H-SiC (0001) substrates were prepared with the donor level of $5 \times 10^{16} \text{ cm}^{-3}$, $5 \times 10^{17} \text{ cm}^{-3}$

or $5 \times 10^{18} \text{ cm}^{-3}$. The wafers were cleaned in hot organic solvents. This step was followed by chemical etching prior to metal deposition: (i) 10 min. in $\text{NH}_4\text{OH}:\text{H}_2\text{O}_2:\text{H}_2\text{O} = 1:1:5$ at 65 °C, (ii) 10 min. in $\text{H}_2\text{O}_2:\text{HCl}:\text{H}_2\text{O} = 1:1:5$ at 70 °C; (iii) 2 min. in $\text{HF}:\text{NH}_4\text{F}:\text{H}_2\text{O} = 2:7:1$. Titanium or nickel metallization with thickness of 100 nm was formed using the *lift off* technique and deposition by DC magnetron sputtering at room temperature from elemental targets of 99.99 % purity in Ar plasma. Circular Transmission Line Model (c-TLM) was chosen for calculation of specific contact resistance. The ohmic contacts were formed by Rapid Thermal Annealing (RTA) process under argon within the temperature range of 950–1100 °C for 3 min.

Table 1. The influence of annealing temperature and doping level on the specific contact resistance.

T [°C]		Specific contact resistance [Ωcm^2]		
		$5 \times 10^{16} \text{ cm}^{-3}$	$5 \times 10^{17} \text{ cm}^{-3}$	$5 \times 10^{18} \text{ cm}^{-3}$
Ni	1000	non-ohmic	1.2×10^{-4}	3.9×10^{-5}
	1050	1.8×10^{-4}	9.0×10^{-5}	8.0×10^{-6}
Ti	1000	non-ohmic	non-ohmic	4.2×10^{-4}
	1050	4.1×10^{-4}	4.3×10^{-4}	1.2×10^{-4}
	1100	3.1×10^{-4}	2.2×10^{-5}	8.9×10^{-5}

The specific contact resistance was calculated from I - V characteristics. To study the current transport mechanism at the n-SiC/metal interface, the characteristics were measured by Keithley 2400 Source-Meter within the temperature range of 20–300 °C. Finally, the Arrhenius plots were prepared for each concentration level to determine the transport mechanism. The diffraction data were collected using a Philips X'Pert Alpha1 Pro diffractometer equipped with a Ge incident-beam monochromator and a strip detector.

3. Results

For all three doping levels, the as-deposited nickel or titanium layers on SiC formed Schottky contacts with the barrier height of 1.6 eV and 0.78 eV, respectively. The ohmic contacts were formed by RTA process in argon at temperature range of 950 ÷ 1050 °C for nickel and 950 ÷ 1100 °C for titanium. The I - V characteristics for Ni- and Ti-based contacts for different doping concentration and annealing temperatures were shown in Fig. 1. The values of the specific contact resistance for both Ni and Ti metallizations as a function of doping level and annealing temperature are gathered in Table 1.

The linearization of ohmic contact I - V characteristics after RTA process is initiated at temperature of 1000 °C for higher doping levels only ($n = 5 \times 10^{17} \text{ cm}^{-3}$ for Ni and $5 \times 10^{18} \text{ cm}^{-3}$ for Ti). When the annealing temperature increases up to 1050 °C, the I - V characteristics become linear. It indicates the ohmic behavior in the whole analyzed doping range. The reduction of the specific

contact resistance for Ti/SiC contacts is observed after annealing at 1100 °C. Ni/SiC contacts annealed at this temperature reveal increased contact resistivity and worse surface morphology. The lowest values of the specific contact resistance for Ni and Ti contacts formed on n-SiC with carrier concentration of $5 \times 10^{18} \text{ cm}^{-3}$ were 8.0×10^{-6} and $8.9 \times 10^{-5} \Omega\text{cm}^2$, respectively. For low doped SiC the contact resistivity was $3.1 \times 10^{-4} \Omega\text{cm}^2$ for Ti and $1.8 \times 10^{-4} \Omega\text{cm}^2$ for Ni contact at room temperature. The study confirms that the ohmic contact formation on n-SiC layer with higher concentration takes place at lower temperature. It is found that for all three doping levels, the ohmic contacts form through annealing at the temperature of 1050 °C. For Ti-based metallization, the contact resistivity was reduced after annealing at 1100 °C. The X-ray diffraction patterns were obtained for both metallization systems and the results are shown in Fig. 2. Only Ni₂Si phase was detected in the XRD diffractogram after annealing of the Ni/SiC contact at 1050 °C. The Ni₂Si phase is known to be the most thermodynamically stable silicide within the group of nickel silicides. Two compounds were detected in the case of Ti/SiC contact after annealing at 1100 °C: Ti₅Si₃ and Ti₈C₃. The Bragg peaks from Ti₅Si₃ and Ti₈C₃ are displayed in Fig. 2b. The Ti₅Si₃ phase is the dominating compound in the crystalline form.

The mechanism of carriers transport in Ni/n-SiC and Ti/n-SiC ohmic contacts was investigated by the analysis of annealing temperature influence on the specific contact resistance. The results are presented in Fig. 3. As it was already mentioned, the ohmic contacts were formed at 1050 °C and 1100 °C for Ni

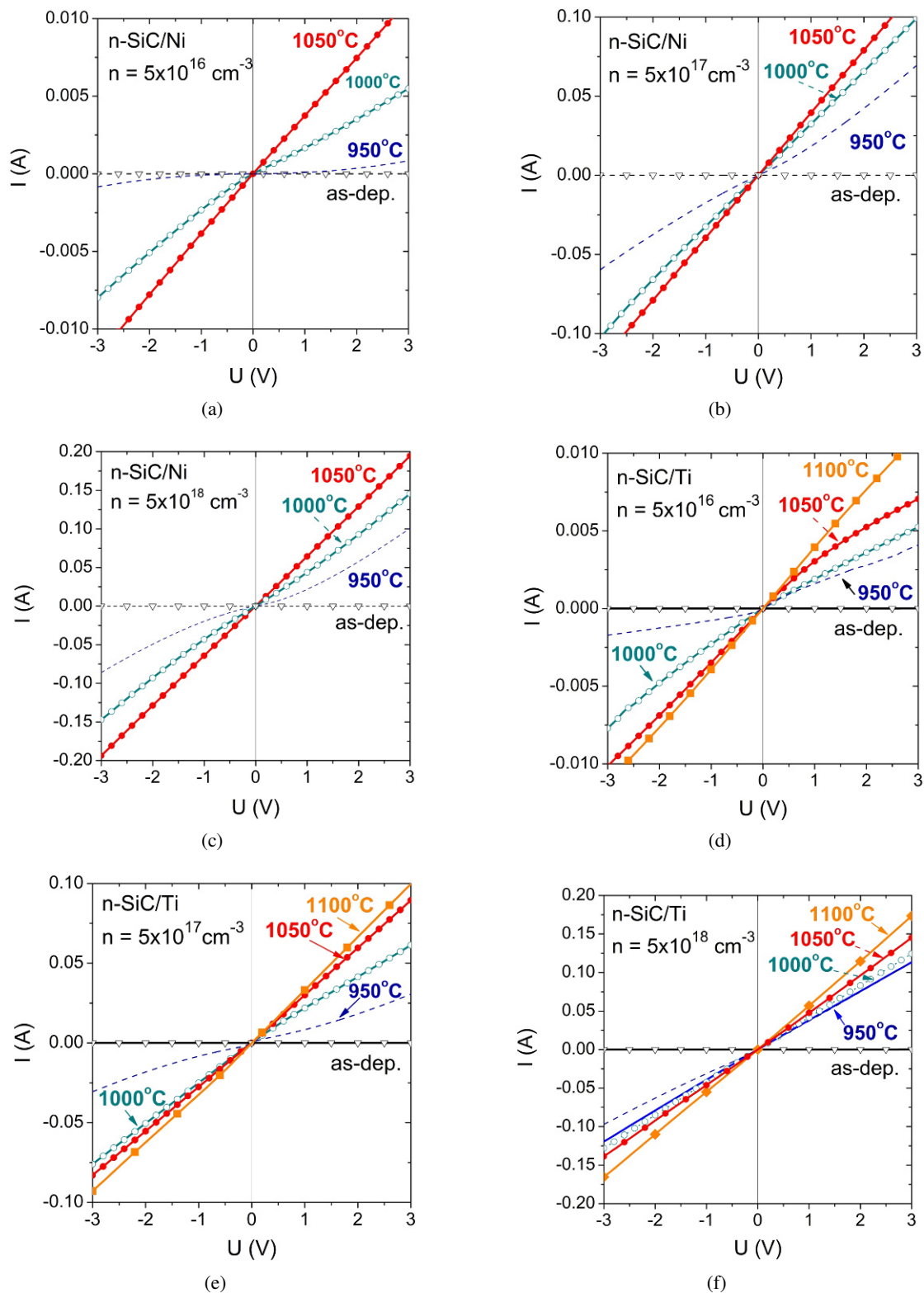


Fig. 1. The dependence of I - V characteristics for Ni- (a, b and c) and Ti- based (d, e and f) contacts metallization for various dopant concentration levels, the samples being annealed at temperatures in the range of 950 °C–1100 °C.

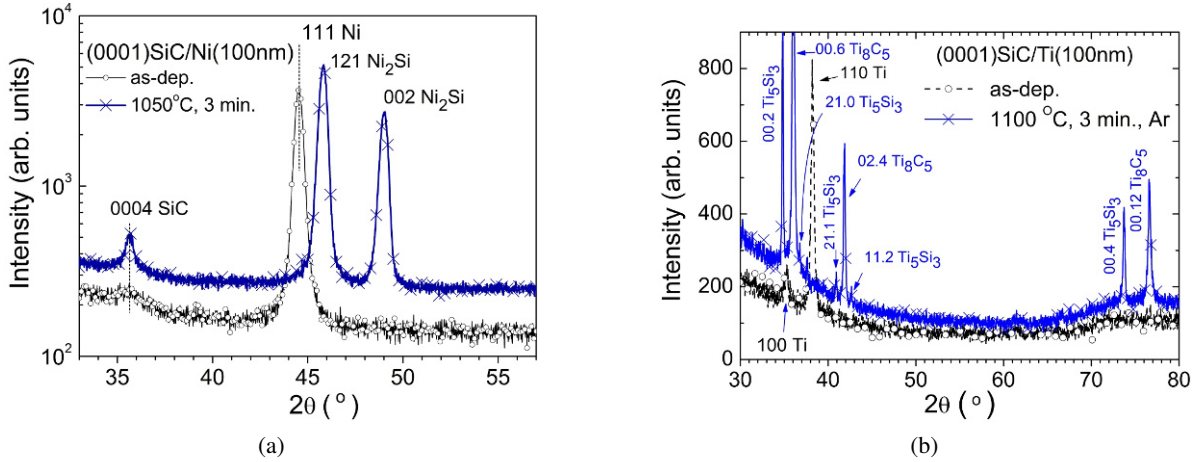


Fig. 2. The X-ray diffraction spectra of the Ni/SiC (a) and Ti/SiC (b) contacts before and after annealing.

and Ti, respectively. The dependence of r_c on temperature is well-defined for the contacts deposited on low doped substrates. The r_c value decreases from 1.8×10^{-4} to the value below $1 \times 10^{-5} \Omega\text{cm}^2$ for Ni and from 3.1×10^{-4} to $8.9 \times 10^{-5} \Omega\text{cm}^2$ for Ti. This proves that the thermionic emission is the predominant mode of the conduction. The barrier heights calculated from Arrhenius plot are 270 and 290 meV for Ti and Ni contacts, respectively. For moderate doping concentrations and thermionic-field emission the contact resistivity decreases to the level of $10^{-5} \Omega\text{cm}^2$. The faster decrease at the temperature about 200 °C is visible. The barrier heights calculated from Arrhenius plot are 157 and 130 mV for Ti and Ni contacts, respectively. For the highest dopant concentration ($n = 5 \times 10^{18} \text{ cm}^{-3}$) a weak dependence of the specific contact resistance r_c versus temperature T is observed and the predominant mode of the conduction is the field emission. The r_c value of $8.0 \times 10^{-6} \Omega\text{cm}^2$ for Ni and $8.9 \times 10^{-5} \Omega\text{cm}^2$ for Ti contacts was calculated.

4. Discussion

The formation of nickel or titanium silicide after metal deposition on silicon carbide surface involves the free silicon atoms from the substrate. The specific activation energy is indispensable to overcome the silicon carbide bonds strength. The decomposition energy is extremely high for silicon carbide itself. The decomposition process is strongly acti-

vated by chemical reaction and enhanced by penetration of metal atoms into silicon carbide subsurface as a result of the difference in the thermal expansion coefficients between the film material and the substrate material. Generally, most of the applied metals are characterized by higher thermal expansion coefficient in comparison to silicon carbide which generates the compression of the metal film and a tension of semiconductor subsurface. The influence of the nickel migration into silicon carbide on chemical bonding strength has been investigated and modelled by others [9]. The impurity atoms in the silicon carbide lattice weaken the covalent bonds. Moreover, the migration process is limited by high hardness of silicon carbide. When the activation energy is overcome, the silicon carbide decomposition leads to silicon and carbon diffusion into nickel film. The first stage of the silicide formation is fully controlled by the silicon atoms supply from the silicon carbide subsurface. Next, the mixture of silicon, carbon and nickel atoms is created at the interface. The specific thermal energy is necessary to form the stable silicides or carbides again. The temperature around 500 °C is enough to create the stable form of nickel silicide (Ni_2Si) [10] which is the basic step of the ohmic contact formation. However, the average barrier height between Ni silicides and silicon carbide is still too high to create ohmic contact. The barrier height approaching the value of 1.3 eV for $\text{Ni}_2\text{Si}/\text{SiC}$ contact was published by F. La Via *et al.* [11]. The growing silicide film creates a barrier

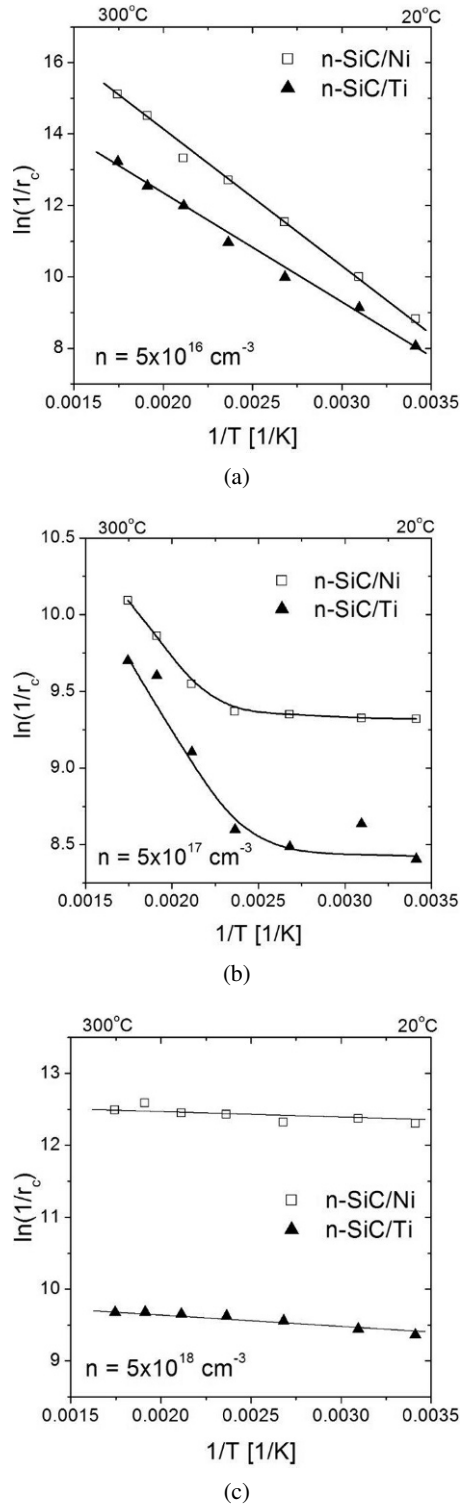


Fig. 3. The dependence of specific contact resistance on temperature in form of Arrhenius plot for Ni/ n -SiC and Ti/ n -SiC ohmic contacts at electron concentration of $5 \times 10^{16} \text{ cm}^{-3}$ (a), $5 \times 10^{17} \text{ cm}^{-3}$ (b) and $5 \times 10^{18} \text{ cm}^{-3}$ (c).

for unreacted metal against diffusion into silicon carbide interface. The decrease of metal atoms flux through the silicide layer along the silicide grain boundaries becomes a key factor for determining the reaction rate at silicide and silicon carbide interface, and temperature much higher than 500 °C is necessary to improve the metal diffusion and continue the reaction at the silicide and silicon carbide interface. Simultaneously, the silicide layer limits the carbon atoms out-diffusion to the metal surface which can act as a sink for the carbon species. The accumulation level of the carbon atoms on the external surface depends on temperature and ambient conditions, while the efficiency of the carbon elimination from the external surface depends mainly on carbon oxidation rate.

The contact formation process is more complex for titanium which creates stable form of carbide (Ti_8C_5). The carbon species coming from silicon carbide decomposition diffuse through the growing titanium silicide layer (Ti_5Si_3) leading to formation of titanium carbide. The titanium carbide film prevents outmigration of carbon and acts as additional diffusion barrier against migration of titanium into the interface [12]. The annealing temperature has to be increased for diffusion rate improvement in comparison to nickel silicide formation. Higher contact resistivity of the titanium-based ohmic contact can be explained by harder conditions of the silicide formation but the thermal reliability of the contact is often improved. Moreover, the thin refractory titanium carbide film protects the ohmic contact against undesirable oxidation process at elevated temperature giving an advantage over the NiSi_2 contact.

As mentioned above, the highly conductive silicide formation is an insufficient factor for high quality ohmic contact due to the barrier height between silicide and silicon carbide. The barrier can be lowered by additional intermediate layer created as a result of silicon carbide surface graphitization. The choice of the metallization influences the surface graphitization degree because metals as catalysts decrease the graphitization temperature and accelerate the process [13]. The process is controlled by silicon carbide decomposition rate and by the rate of carbon diffusion within the film. Highly catalytic metals such as nickel penetrate easily to silicon

carbide subsurface, weaken the silicon carbide covalence bondings and create unstable carbides which decompose immediately to form graphite at relatively low temperature around 700 °C [13]. The graphite formation can be supported by limited carbon diffusion like in the case of titanium carbide on titanium silicide film acting as the diffusion barrier. However, the silicide and silicon carbide interface is carbon-depleted in this case due to titanium carbide formation. Simultaneously, the silicide is titanium-depleted due to limited diffusion of metal through the carbide film. Summarizing, the carbide layer itself and the weaker catalytic properties of titanium are expected to cause higher contact resistivity of the titanium-based ohmic contact. The graphitization is more efficient at higher temperatures and the satisfying rate of the process can be achieved at temperature of 900 °C in the catalytic metal presence which seems to be minimum temperature value for formation of low resistivity ohmic contacts. In this work, the surface graphitization at the applied annealing temperature range is fully confirmed by the calculated barrier height for low doped substrates. The calculated value of 0.3 eV is related to graphite and n-type Si-face silicon carbide interface [14]. The analysis of low doped substrates confirms that the intermediate graphite film itself is insufficient to form the ohmic contact of the lowest resistivity, again. The moderate specific contact resistance value of $10^{-4} \Omega\text{cm}^2$ was obtained for these substrates. The electron tunneling efficiency is not satisfactory for the ohmic contacts on low doped silicon carbide. The calculated value of the barrier height is markedly lower than 0.3 eV for medium and high doped substrates. It means that a different mechanism determines the barrier height and the specific contact resistance of the ohmic contact.

The carbon vacancy mechanism was reported by many authors as an explanation of the barrier lowering [15]. The donor-like carbon vacancies increase the electron concentration in the near interface region changing the electrical properties of the intimate contact between graphite intermediate layer and silicon carbide surface. The clearly observed the barrier height lowering can be indeed enhanced by the thermionic field-emission, which is a result of graphite disorder and inhomogeneity [16, 17].

This work confirms the dependence of the barrier height value on the dopant concentration level. It is possible that the nitrogen atoms may play an important role for the generation of interface states, donor-like vacancies or graphite disorder. However, the redistribution of nitrogen during silicide and graphite film formation can be expected. The extremely thin nitrogen-rich layer can be piled up in front of the graphite and silicon carbide interface at applied annealing temperature. The snowplow phenomenon has been investigated in details for silicon substrates [18]. The shallow peak of the impurity concentration can be obtained at relatively low temperature in comparison to standard doping processes. The substitutional nitrogen atoms distributed over a depth of 1–2 nm contribute to conduction mechanism and lower the barrier height. Additionally, the doping process beneath the interface is consistent with vacancies mechanism. The carbon or silicon vacancies beneath the interface are responsible for substitutional incorporation of nitrogen. The snowplow assumption agrees with the barrier lowering model proposed by Bindell for PtSi and n-type silicon interface [19]. The low contact resistivity is expected as a result of the barrier lowering.

5. Summary

Carriers transport through m-s interface, created by Ni- or Ti-based ohmic contacts, depends strongly on the dopant concentration level. It was found, that for both Ni/n-SiC and Ti/n-SiC ohmic contact structures with low dopant concentration of $5 \times 10^{16} \text{ cm}^{-3}$ the contact resistivity strongly depends on measuring temperature. It suggests strongly, that the carriers transport has thermionic emission nature. For samples with dopant concentration of $5 \times 10^{17} \text{ cm}^{-3}$ the thermionic emission was identified as the dominant transport mechanism at temperatures exceeding 200 °C. For SiC with dopant concentration of $5 \times 10^{18} \text{ cm}^{-3}$ the contact resistivity is weakly temperature-dependent and the carriers transport has mainly field emission character.

It was suggested that donor-like carbon vacancies as well as an accumulation of nitrogen at the interface may be responsible for lowering the bar-

rier height below 0.3 eV and the decrease in the specific contact resistance. Lowering the barrier by graphite disorder and inhomogeneity at the interface has been confirmed by other researches. However, the chemical analysis of the interfacial region using XPS and SIMS depth profiles is recommended to justify the explanation. The characterization is a subject of continuing investigation.

Acknowledgements

The research was partially supported by the European Union within European Regional Development Fund, through grant Innovative Economy (POIG.01.03.01-00-159/08, "In-TechFun"). The authors are grateful to W. Strupinski from "Epi-Lab" Semiconductor Compounds Epitaxy Laboratory at Institute of Electronic Materials Technology (ITME) in Warsaw for epitaxial layers deposition.

References

- [1] PORTER L.M., DAVIS R.F., *Mater. Sci. Eng.*, B34 (1995), 83.
- [2] CHANG S-C., WANG S-J., UANG K-M., LIOU B-W., *Solid State Electronics*, 49 (2005), 1937.
- [3] BLANK T.V., GOL'DBERG YU.A., *Semiconductors*, 41 (2007), 1263.
- [4] PADOVANI F.A., STRATTON R., *Solid State Electron.*, 9 (1966), 695.
- [5] RHODERICK E. H., *Metal-Semiconductor Contacts*, Clarendon, Oxford, 1978.
- [6] PECZ B., TO' TH L., DI FORTE-POISSON M., VACAS J., *Appl. Surf. Sci.*, 206 (2003), 8.
- [7] WANG Z., TSUKIMOTO S., MITSUHIRO S., KAZUHIRO I., MURAKAMI M., IKUHARA Y., *Phys. Rev.*, B 80 (2009), 245303.
- [8] NIKITINA I.P., VASSILEVSKI K.V., WRIGHT N.G., HORSFALL A.B., O'NEILL A.G., JOHNSON C.M., *J. Appl. Phys.*, 97 (2005), 083709.
- [9] YURYEVA E.I., IVANOVSKII A.L., *Russ. J. Coord. Chem.*, 28 (2002), 881.
- [10] KURIMOTO E., HARIMA H., TODA T., SAWADA M., IWAMI M., NAKASHIMA S., *J. Appl. Phys.*, 91 (2002), 10215.
- [11] LA VIA F., ROCCAFORTE F., MAKHTARI A., RAINERI V., MUSUMECI P., CALCAGNO L., *Microelectronic Eng.*, 60 (2002), 269.
- [12] LEVIT M., GRIMBERG I., WEISS B.-Z., *J. Appl. Phys.*, 80 (1996), 167.
- [13] WEIJIE L., MITCHEL W.C., LANDIS G.R., CRENSHAW T.R., COLLINS W.E., *J. Appl. Phys.*, 93 (2003), 5397.
- [14] SEYLLER TH., EMTSEV K.V., SPECK F., GAO K.-Y., LEY L., *Appl. Phys. Lett.*, 88 (2006), 242103.
- [15] HAN S.Y., KIM K.H., KIM J.K., JANG H.W., LEE K.H., KIM N.-K. KIM E.-D., LEE J.-L., *Appl. Phys. Lett.*, 79 (2001), 1816.
- [16] WEIJIE L., MITCHEL W.C., THORNTON C.A., LANDIS G.R., COLLINS W.E., *J. Electronic Mat.*, 32 (2003), 426.
- [17] TUNG R.T., *Mat. Sci. Eng.*, R35 (2001), 1.
- [18] WITTMER M., TING C.-Y., OHDOMARI I., TU K.N., *J. Appl. Phys.*, 53 (1982), 6781.
- [19] BINDELL J.B., MOLLER W.M., LABUDA E.F., *IEEE Trans. Electron Devices*, ED-27 (1980), 420.

Received 21.12.2010

Accepted 18.12.2011